Indian National Centre for Ocean Information Services (INCOIS)

Ministry of Earth Sciences, Govt. of India
Hyderabad-500090

INCOIS/ENSO/Special/Bull/2026/06 **15th November 2026**

Special El Niño Outlook Bulletin

Highlights:

- **Sea surface temperature anomalies over the central and eastern equatorial Pacific indicate further strengthening of El Niño conditions during October 2026, with the Niño 3.4 index reaching approximately +3.0°C, accompanied by strong subsurface warming exceeding +4°C in several areas.**
- **The INCOIS forecast indicates El Niño as the dominant ENSO phase from November 2026 to March 2027, with probabilities ranging from approximately 87% to 100%. ENSO-neutral conditions are expected to dominate during April-June 2027, followed by an increasing probability of La Niña conditions from June-August 2027 onwards.**
- **Marine heatwave-affected areas increased substantially in both the Arabian Sea and the Bay of Bengal during 2026 compared with 2025. During October-November 2026, the affected area reached approximately 80-90% in the Arabian Sea, while the Bay of Bengal also experienced widespread marine heatwave conditions.**
- **Coastal upwelling along the southwest coast of India was weaker during May-July 2026 compared with 2025, followed by an increase during August-September. The Indian Ocean Dipole index remained above the +0.4°C threshold from July to October 2026, indicating persistent positive IOD conditions.**
- **Persistent ocean warming and changes in coastal upwelling may influence marine productivity, fish habitats and the distribution and availability of commercially important fish species, including Indian Oil Sardine and Indian Mackerel.**
- **Fishermen, maritime operators and coastal communities are advised to monitor**

INCOIS ocean services, including Potential Fishing Zone advisories, Ocean State Forecasts, Marine Heatwave Advisories, High Wave Alerts and other coastal hazard advisories.

Introduction

El Niño refers to the warming of the eastern Pacific Ocean associated with the positive phase of the El Niño-Southern Oscillation (ENSO). A prevailing El Niño condition in the Pacific Ocean has an adverse effect on the Indian summer monsoon rainfall and, thereby, on the economic well-being of the country. El Niño is also found to cause stronger and prolonged marine heatwaves in the northern Indian Ocean, damaging the ecological balance, coral reefs and causing significant losses to the fishery industry. Thus, monitoring the El Niño condition and predicting its further evolution with sufficient lead time is of prime importance for better preparedness and policymaking.

Beyond its influence on monsoon rainfall, El Niño can significantly alter ocean conditions across the Indian Ocean through changes in sea surface temperature, upper-ocean heat content, ocean circulation, marine heatwaves, and marine ecosystem productivity. These changes can influence fisheries, coral reef health, coastal hazards, and maritime activities, making ENSO outlooks valuable for a range of operational ocean services provided by INCOIS. This bulletin outlines the current state of the Pacific Ocean and an outlook on the evolution of El Niño/La Niña conditions in the subsequent seasons.

Details of the datasets and methodology used to prepare this bulletin are given in Annexure-I.

Evolution of Niño 3.4 Sea Surface Temperature Anomaly

The monthly evolution of Niño 3.4 SST anomalies during the past two years is shown in Fig. 1. La Niña conditions prevailed during the second half of 2025, with negative SST anomalies reaching approximately −1.3°C during September-November 2025. Subsequently, the cooling weakened, and ENSO-neutral conditions developed during February-April 2026. Positive SST anomalies emerged in May 2026 and strengthened progressively, reaching approximately +3.0°C by October 2026 (Fig. 1), indicating the development of strong El Niño conditions. Figure 2 illustrates the evolution of surface and subsurface temperature anomalies across the tropical Pacific during October 2025, January 2026, April 2026 and July 2026. Pronounced subsurface warm anomalies developed in the western equatorial Pacific during October 2025. These anomalies subsequently extended eastward during early 2026, reaching the central and eastern equatorial Pacific by April 2026. By July 2026, strong subsurface warming extended across much of the central and eastern equatorial Pacific, accompanied by the development and strengthening of positive SST anomalies in the central and eastern Pacific. As shown in Fig. 3, by October 2026, marked positive SST anomalies exceeding +3°C were observed across the

central and eastern equatorial Pacific. Strong subsurface warm anomalies, exceeding +4°C in several areas, extended across a substantial portion of the central and eastern equatorial Pacific. The simultaneous presence of strong surface and subsurface warming indicates the continued intensification of El Niño, with strong El Niño conditions prevailing during October 2026.

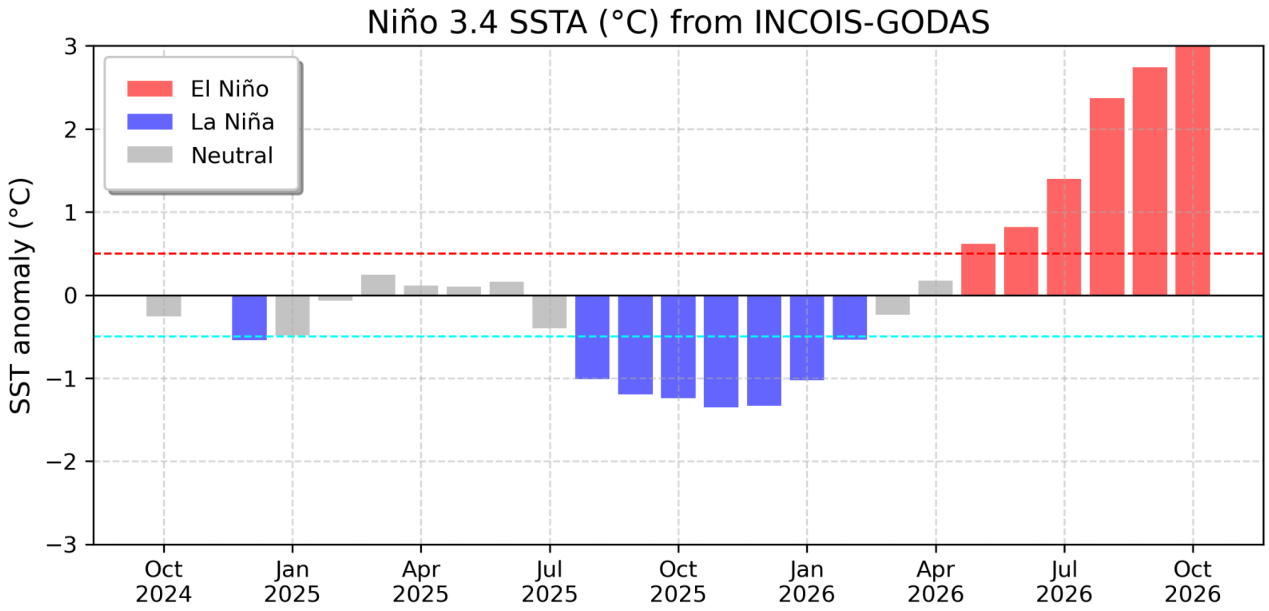


Fig. 1: Evolution of monthly sea surface temperature anomalies (SSTA, °C) in the Niño 3.4 region (5°S-5°N, 170°W-120°W) from October 2024 to October 2026. The red and cyan horizontal lines indicate the +0.5°C and −0.5°C anomaly thresholds, respectively, used to identify El Niño and La Niña conditions.

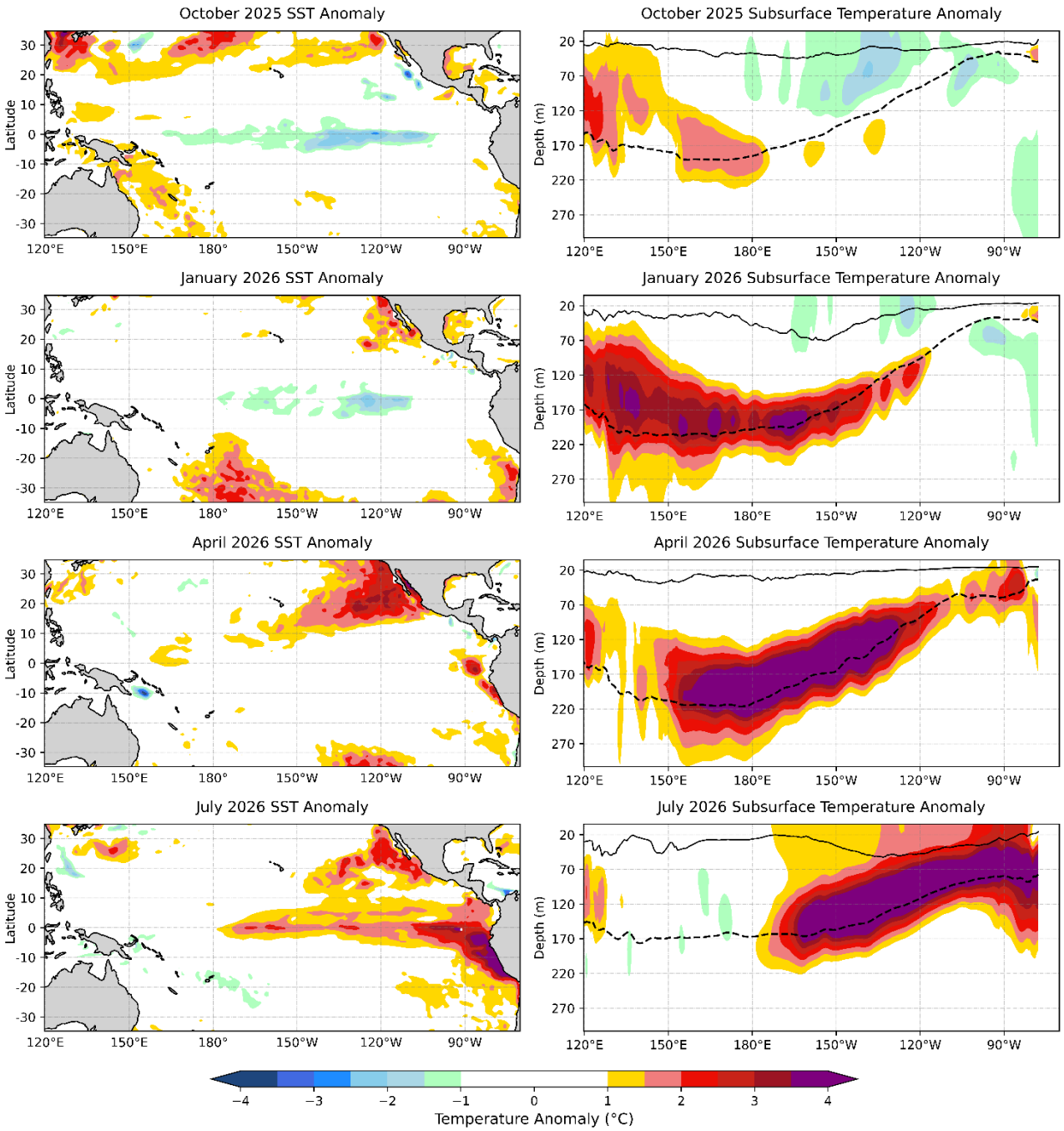


Fig. 2: Evolution of sea surface and subsurface temperature anomalies in the tropical Pacific during October 2025, January 2026, April 2026 and July 2026. The left panels show monthly sea surface temperature anomalies, while the right panels show subsurface temperature anomalies averaged over 5°S-5°N.

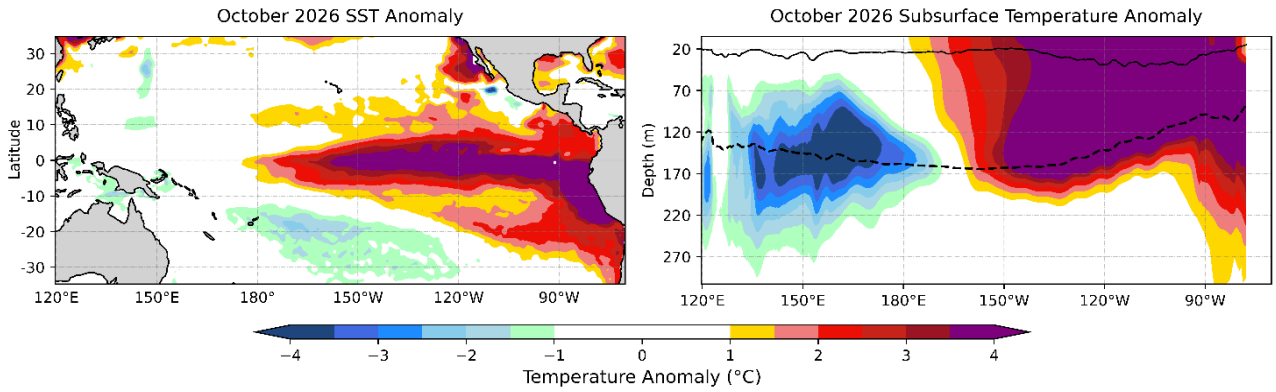


Fig. 3: Sea surface and subsurface temperature anomalies in the tropical Pacific during October 2026. The left panel shows the monthly sea surface temperature anomaly, while the right panel shows the subsurface temperature anomaly averaged over 5°S-5°N.

INCOIS Outlook for Niño 3.4 index

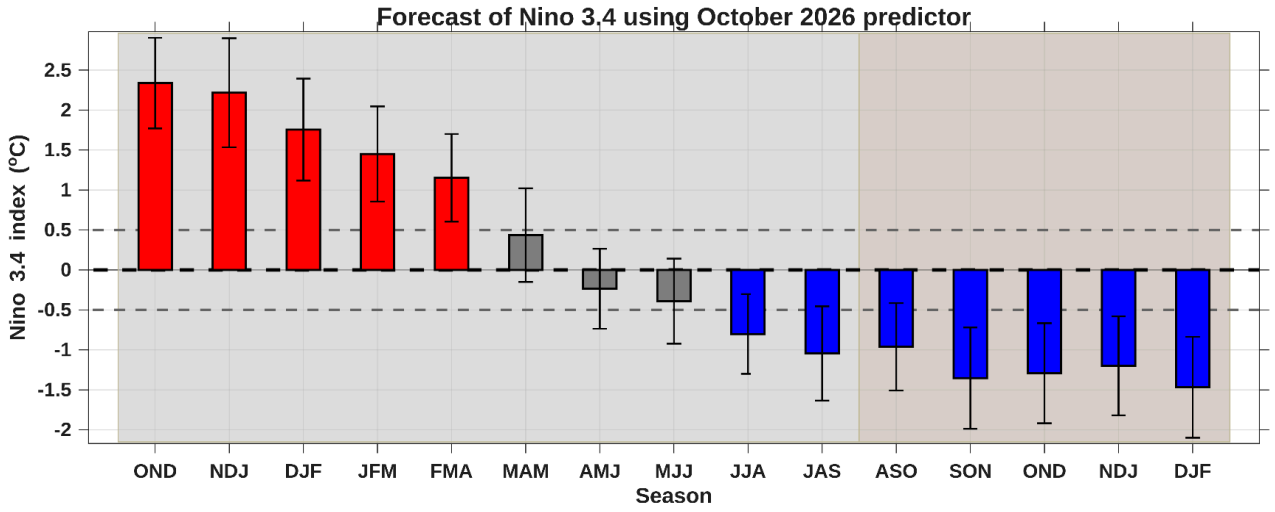


Fig. 4: Median forecast of the Niño 3.4 index for the upcoming seasons, based on August-October 2026 predictors. The error bars indicate the spread of the model predictions.

INCOIS has developed a deep learning-based Bayesian Convolutional Neural Network (BCNN) model to provide probabilistic outlooks of the future evolution of the Niño 3.4 index. The model provides skillful predictions of the Niño 3.4 index up to a lead time of 15 months [See Annexure-I for more details of the model and its skill levels]. Median values of Niño 3.4 SST anomalies predicted by the model based on the August-October 2026 initial conditions extracted from INCOIS-GODAS are shown in Fig. 4. The forecast indicates that El Niño conditions are expected to persist from November 2026 to March 2027, with median Niño 3.4 SST anomalies remaining well above the +0.5°C threshold. The probability of El Niño remains high during this period, ranging from approximately 87% to 100% (Fig. 5). Subsequently, the Niño 3.4 index is

projected to weaken, with ENSO-neutral conditions becoming dominant during April-June 2027, reaching a probability of approximately 64% during April-June and remaining the most likely phase in May-July 2027. La Niña conditions are expected to emerge as the dominant phase from June-August 2027 onwards, with probabilities increasing to approximately 70%-90% during the later forecast seasons. The median forecast also indicates a transition towards negative Niño 3.4 SST anomalies during the second half of 2027, suggesting the possible development of La Niña conditions.

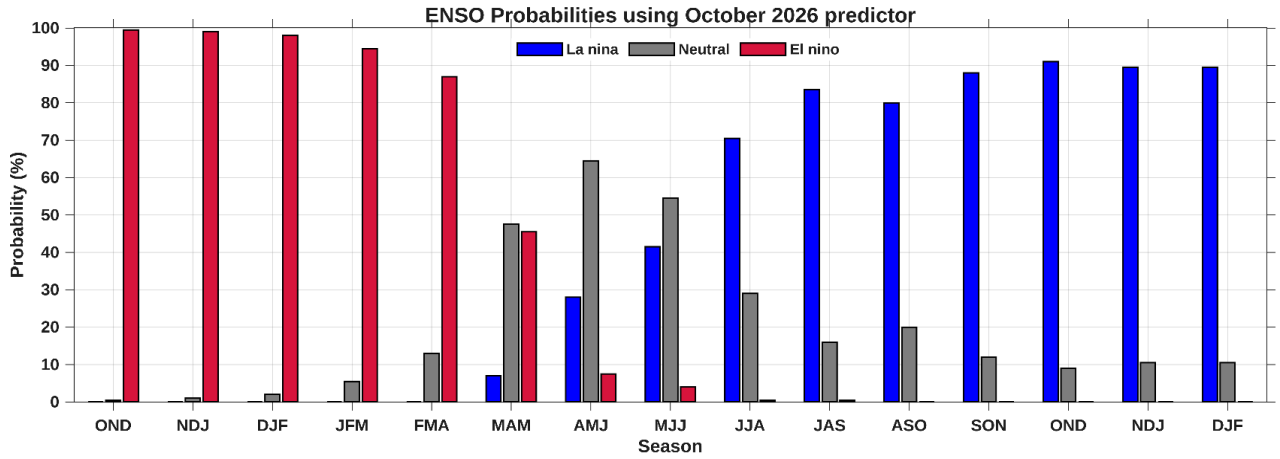


Fig. 5: Forecast probabilities of El Niño, La Niña and ENSO-neutral conditions for the upcoming seasons, based on August-October 2026 predictors.

Impact of El Niño on the maritime sectors in Northern Indian Ocean

Strong El Niño conditions prevailing over the equatorial Pacific are expected to influence ocean conditions across the Northern Indian Ocean during the upcoming seasons. The associated changes in ocean temperature and circulation, together with evolving Indian Ocean conditions, may influence marine heatwaves, coastal upwelling, marine productivity and fisheries. These changes require continued monitoring to assess their potential implications for marine ecosystems and maritime activities.

- *Marine heatwave (MHW) conditions:* The spatial extent of marine heatwaves in 2026 has increased substantially compared with 2025 in both the Arabian Sea and the Bay of Bengal (Fig. 6). In the Arabian Sea, the MHW-affected area increased considerably from March 2026 onwards, with a sharp and sustained expansion during September-November, reaching approximately 80-90% of the region. In the Bay of Bengal, the affected area also increased during the second half of 2026, reaching approximately 85-90% during October, before remaining relatively high in November. In comparison, MHW-affected areas during several months of 2025 were generally lower, particularly during the latter part of the year. The persistence and expansion of these warm conditions may increase thermal stress on marine ecosystems and coral reefs, raising the likelihood of coral bleaching during prolonged marine heatwave events.

- *Coastal upwelling:* Monthly Coastal Upwelling Transport Index (CUTI) values along the southwest coast of India indicate differences in the seasonal evolution of upwelling between 2025 and 2026 (Fig. 7). Upwelling during 2026 was weaker than in 2025 during May-July, with the most noticeable difference observed in July, when the 2025 index reached its seasonal maximum. However, the index increased during August 2026, reaching values slightly higher than those observed in August 2025, and remained comparable during September. Upwelling weakened considerably in October in both years. These variations indicate a weaker peak-season upwelling signal in 2026, followed by an increase during the later part of the upwelling season.

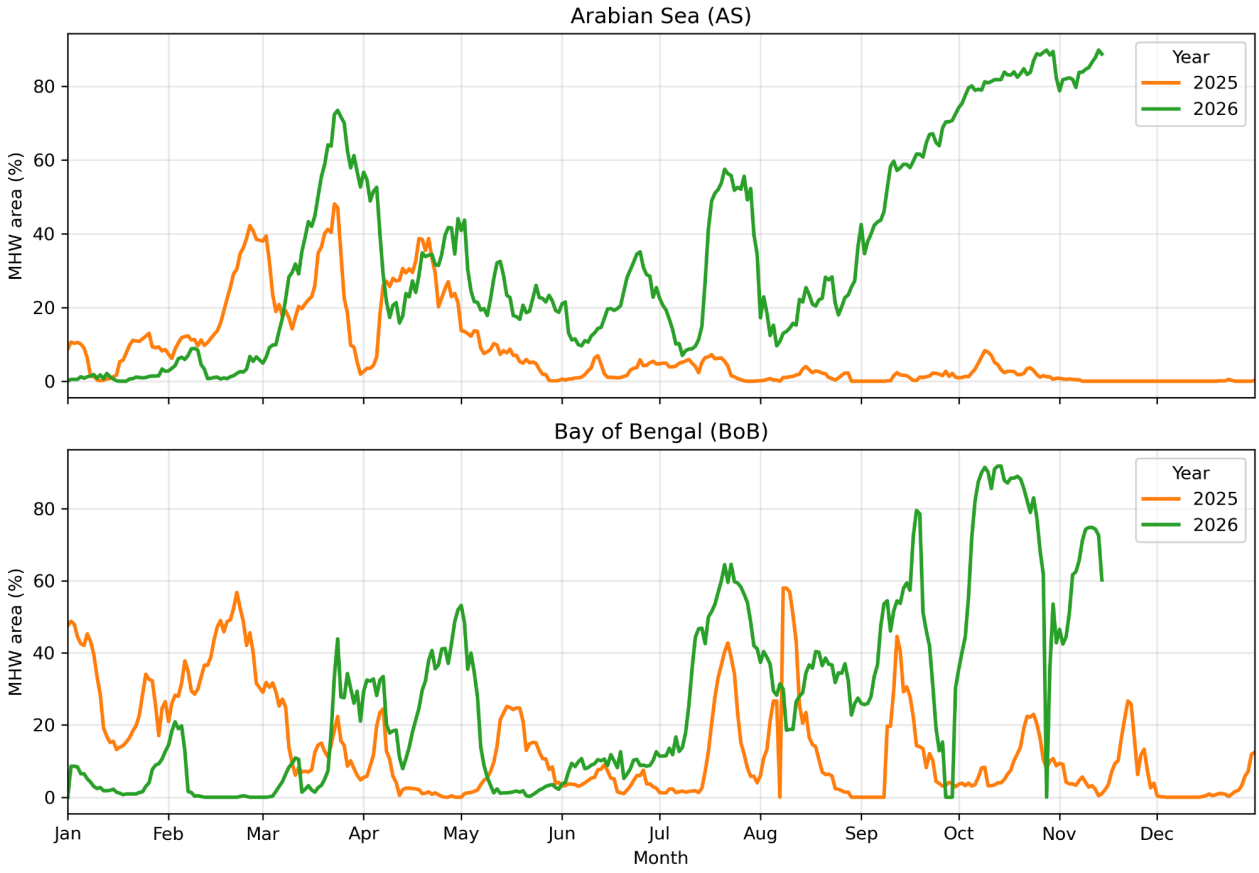


Fig. 6: Comparison of marine heatwave-affected areas in the Arabian Sea and Bay of Bengal during 2025 and 2026.

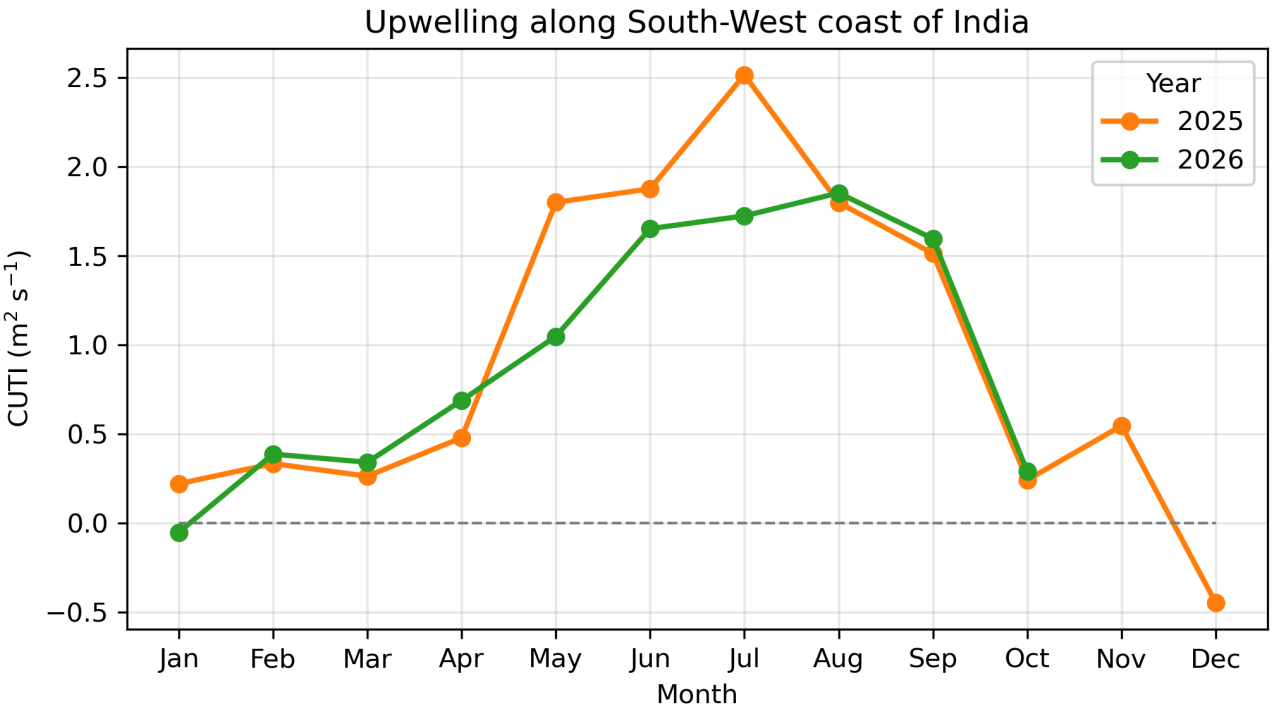


Fig. 7: Monthly variation in coastal upwelling along the southwest coast of India, showing weaker peak-season upwelling in 2026 compared with 2025.

- *Indian Ocean Dipole (IOD):* The IOD index shows a clear development of positive IOD conditions during 2026 (Fig. 8). After remaining close to neutral during much of the first half of the year, the index increased above the +0.4°C threshold in July and remained positive during August and September. It weakened slightly in September before strengthening again in October 2026. In contrast, predominantly negative IOD conditions prevailed during the second half of 2025, with the index reaching approximately −1.35°C in October. The development and persistence of positive IOD conditions during the second half of 2026 indicate a marked contrast in Indian Ocean conditions between the two years. Continued monitoring of the IOD is important for understanding its evolving influence on regional ocean and climate conditions.
- *Fisheries and marine productivity:* Persistent warming and changes in coastal upwelling may influence nutrient availability, marine productivity, and fish habitats. These changes may affect the distribution and availability of commercially important fish species, including Indian Oil Sardine and Indian Mackerel, during the upcoming fishing season.
- *Ocean services and preparedness:* Changes in ocean temperature and marine productivity associated with persistent warming may affect fishing conditions and the distribution of Potential Fishing Zones during the upcoming seasons.

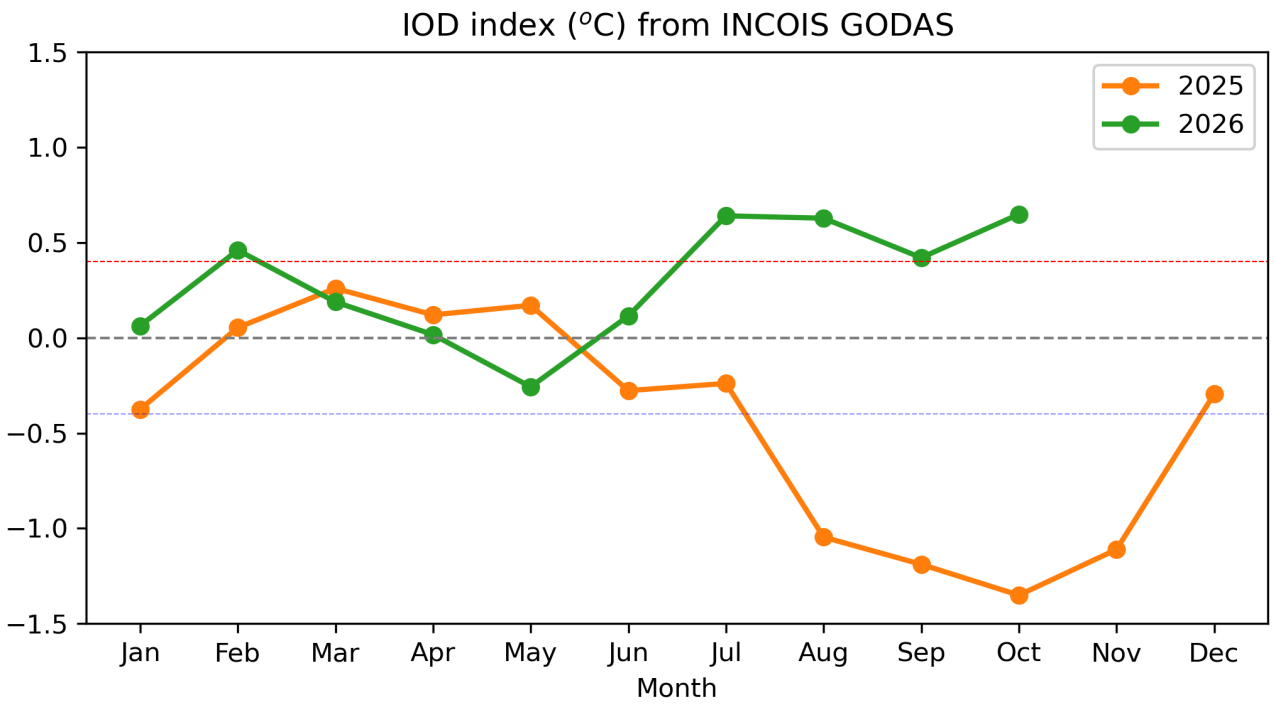


Fig. 8: Indian Ocean Dipole (IOD) conditions during 2025 and 2026, showing a strengthening positive IOD signal.

- Warmer ocean conditions may influence the background environment for extreme weather events, while coastal regions may remain vulnerable to localized erosion, flooding and storm-surge impacts during severe weather episodes.
- Fishermen, maritime operators, coastal communities, tourism stakeholders and disaster-management agencies are advised to closely monitor INCOIS ocean services throughout the forecast period, including Potential Fishing Zone advisories, Ocean State Forecasts, High Wave Alerts, Swell Advisories, Storm Surge Forecasts and Coastal Inundation Services.
- INCOIS will continue to provide Marine Heatwave Advisory System (MAHAS), Ocean State Forecasts (OSF), Coral Bleaching Alerts and Harmful Algal Bloom (HAB) advisories to support preparedness and decision-making during the evolving El Niño conditions.

DISCLAIMER: This bulletin is based on numerical ocean model and ML method being run at INCOIS and the conclusions are based on the scientific understanding of those who prepared the bulletin. The predictions are evaluated routinely with available observational datasets. Individuals/groups/organizations are advised to be cautious while taking any decisions based on this bulletin.

Annexure-1

Data and Methodology

INCOIS-GODAS

INCOIS-GODAS is an ocean analysis system based on the Modular Ocean Model (MOM4p0) with 0.5^{o} uniform zonal and varying (0.25 ^{o} at the equator) meridional resolution and 40 vertical z-coordinate levels. It assimilates in-situ temperature and salinity profiles using 3DVAR assimilation scheme. Additionally, the model SST is relaxed to OISST with a 5-day timescale and the surface salinity is relaxed to World Ocean Atlas at a monthly timescale. The model is forced with 6-hourly atmospheric fluxes from GFS v13 (provided by NCMRWF). The analysis is available from 1999 to date.

Bayesian Convolutional Neural Network (BCNN) model that provides probabilistic predictions for El Niño/La Niña conditions.

The advent of deep learning-based approaches marks a transformative era in climate and weather prediction. Here, we introduce a deep learning-based Bayesian Convolutional Neural Network (BCNN) model that provides probabilistic predictions for El Niño/La Niña with a lead time of up to 24 months. The Bayesian layers within the CNN maintain the capability to predict a distribution of learned parameters. The inherent capacity for uncertainty modelling enhances the reliability of BNNs, making them particularly valuable in operational services. Validation of the all-season correlation skill of the Niño 3.4 index from the BCNN model demonstrates significantly higher accuracy up to 16 months leads compared to current state-of-the-art dynamical forecast systems.

Data & Methods:

This work is inspired by the recent study of Ham et al., 2019, in which El Niño/La Niña prediction was carried out using a CNN network and ocean predictors with a lead time of 2 years in advance. A significant drawback of their system was the absence of model uncertainty quantification and confidence in prediction, which has been addressed here using BCNN.

BCNN Model Predictors and training

The prediction approach relies on the fact that El Niño/La Niña is connected to slow oceanic variations and their atmospheric coupling, indicating the potential for early forecast. Here, global, gridded monthly sea surface temperature (SST) data and upper 300 m integrated ocean potential temperature (T0-300) data (at a resolution of 2.5^{0}x2.5^{0}) spanning from 0°-360°E and 55°S-60°N for three consecutive months (n, n-1, n-2) are employed as plausible predictors of El Niño/La Niña, while the predictand or target is the Niño 3.4 index, representing the area-averaged SST anomaly over 170°-120°W and 5°S to 5°N, predicted up to 24 months in advance.

One challenge in applying deep learning to El Niño/La Niña prediction is the scarcity of sufficient training data due to the limited observation period. Since global oceanic temperature records have only been accessible since 1871, fewer than 150 monthly samples are typically available to date. To overcome this limitation, we augment the training dataset by incorporating historical runs (1850-2014 period) from the Coupled Model Intercomparison Project phases 5 (CMIP5) and 6 (CMIP6). CMIP models that exhibit good skill in reproducing historical ENSO characteristics are selected based on previous literature.

The initial training of the model incorporates 11 CMIP5 and 14 CMIP6 models, resulting in a substantial dataset of about 3200 samples. To mitigate systematic errors in the BCNN reflecting those of the CMIP samples, a learning transfer technique was employed, where the fine-tuning of the CMIP pre-trained model was conducted through another training approach utilizing Simple Ocean Data Assimilation (SODA) reanalysis predictors spanning from 1871 to 1980. Details of data are listed in table 1.

Separate BCNN models were set up for each season and each lead time. The BCNN predicted Niño 3.4 index was validated using NCEP-GODAS from 1991-2020. The results show high predictability accuracy, with an all-season correlation skill exceeding 0.8 for the first six months, decreasing to 0.5 after a 16-month lead (see Fig. 9).

Table 1. Details of data used for the BCNN model.

	Data	Period
Training dataset	CMIP5 historical run (11 models)	1850-2005
	CMIP6 historical run (14 models)	1850-2014
Training dataset (Transfer Learning)	Reanalysis (SODA)	1871-1980
Validation dataset	Reanalysis (GODAS)	1990-2020
Operational forecast dataset	INCOIS GODAS	2024 onwards

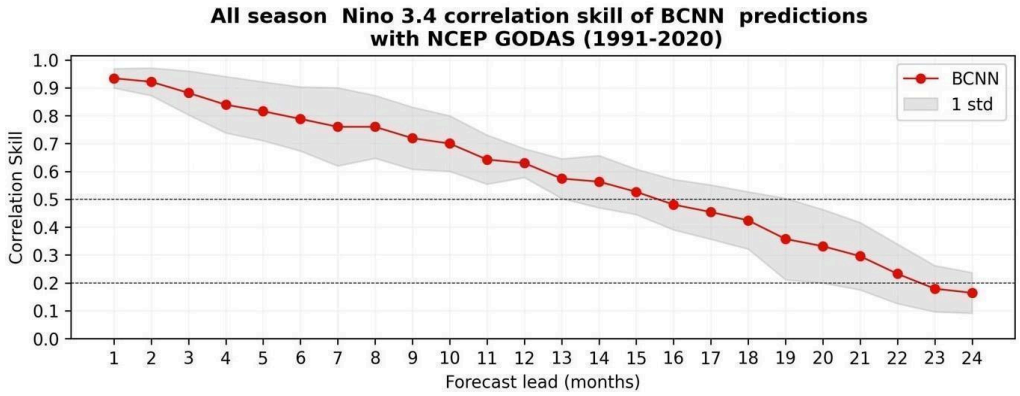


Fig. 9: All-season correlation skill of BCNN-based El Niño/La Niña prediction compared with NCEP-GODAS reanalysis for 1991-2020. The red line represents the median predicted El Niño/La Niña, with the 1 standard deviation of prediction shown in gray shades.

Coastal Upwelling Transport Index

The Coastal Upwelling Transport Index (CUTI) was calculated following the methodology of Jacox et al. (2018), which decomposes the total cross-shore transport into Ekman and geostrophic components. Ocean fields (sea surface height and mixed layer depth) were obtained from the GLORYS12V1 analysis and forecast, while wind stress fields were derived from ERA5 reanalysis. Because the Indian coastline is not uniformly oriented along the north-south axis assumed in the original CUTI formulation, the local coastline-normal direction was estimated at each grid point from the bathymetric gradient, under the assumption that isobaths run approximately parallel to the coast. Wind stress and sea surface height gradients were then projected onto this locally-defined alongshore direction to compute the cross-shore Ekman transport (from the alongshore wind stress) and geostrophic transport (from the alongshore sea surface height gradient scaled by the mixed layer depth), respectively. Daily transport estimates were averaged to monthly resolution, and the resulting CUTI field was spatially masked to the continental shelf (depth < 500 m) prior to regional averaging over the South-West coast of India (70^{o}E-78^{o}E, 5^{o}N-18^{o}N).

Marine Heatwave

A Marine Heatwave (MHW) is defined as a discrete, prolonged, and anomalously warm water event. To be classified as an MHW, the warm water event must persist for five or more consecutive days, with Sea surface temperatures exceeding the 90th percentile of a local 30-year historical baseline and featuring no more than two consecutive days of cooling below this threshold. Here we have used Optimum interpolated Sea Surface temperature data for the present study. The total daily percentage of spatial extent of these MHW covered area was calculated and monitored across two key regions: the Arabian Sea (48.5°E to 77.5°E, 5.0°N to 25.5°N) and the Bay of Bengal (77.5°E to 100.5°E, 5.0°N to 22.5°N).

Fishery impact analysis

Historical analyses of marine fishery landings with the ENSO phases since 1950 indicate that fishery landings across the Indian Ocean region tend to decline during El Niño phases, although the overall decline in catches remains relatively weak and region-specific. To assess the potential implications of ENSO variability for Indian marine fisheries, INCOIS examined the relationships between historical ENSO phases and the landings of major small pelagic species, the Indian Oil Sardine and Indian Mackerel, in their principal landing states of Kerala and Karnataka obtained from CMFRI for the period 1985-2023. The Monthly Climate Timeseries of the Oceanic Niño Index (ONI) V2 (available from NOAA Physical Sciences Laboratory) was used as a measure of the El Niño-Southern Oscillation (ENSO) to compare annual trends in IOS and IM catch with ENSO events. The ONI is calculated as the 3-month running mean of SST anomalies (based on ERSST. v5 data) in the Niño 3.4 region (5°N-5°S, 120°-170°W), using the 197-2000 base period. Spatiotemporal datasets were analyzed with Python (version 3.9.12) libraries and Excel to generate graphical illustrations. Further, relevant literature on the effects of ENSO- driven climate variability on fish life-history processes and fishery productivity was examined to identify the likely consequences of the anticipated El Niño on Indian marine fisheries.

Studies from Indian waters indicate that earlier events of El Niño-induced warming have adversely impacted the maturation of Indian Oil Sardine, while mismatches between phytoplankton productivity and larval feeding requirements reduced recruitment success. Also, climate variability can push fish populations towards their physiological limits, resulting in shifts in distribution towards deeper waters or higher latitudes.

Further, fish growth and size are strongly influenced by food availability and environmental conditions, particularly temperature and productivity changes associated with seasonal precipitation and upwelling. Thus ENSO-driven variability can likely impact the life history traits, especially for the small pelagic species.

Ocean State

El Niño events exert a measurable influence on the surface gravity wave climate of the North Indian Ocean (NIO) through their modulation of monsoon wind systems. Ocean surface waves, which are gravity waves primarily driven by surface winds, are significantly influenced by tropical climate variability modes such as ENSO through changes in surface winds. Over the NIO, this manifests as a spatially asymmetric response between the two sub-basins: ENSO influence on extreme significant wave heights (SWH) includes increases in the Bay of Bengal and decreases in the Arabian Sea, a pattern directly linked to the well-documented weakening of the South Asian monsoon during El Niño years. Strong El Niño events significantly suppress the spatial extent of extreme wind-wave events over the NIO basin.